

Laser-based ultrasound detection using photorefractive quantum wells

I. Lahiri, L. J. Pyrak-Nolte, and D. D. Nolte^{a)}

Department of Physics, Purdue University, 1396 Physics Building, West Lafayette, Indiana 47907-1396

M. R. Melloch

School of Electrical and Computer Engineering, Purdue University, 1285 Electrical Engineering Building, West Lafayette, Indiana 47907-1285

R. A. Kruger

Department of Radiology, Indiana University Medical Center, Indianapolis, Indiana 46202

G. D. Bacher and M. B. Klein

Lasson Technologies, 1331 Avenida de Cortez, Pacific Palisades, California 90272

(Received 16 February 1998; accepted for publication 23 June 1998)

We demonstrate a laser-based adaptive ultrasonic homodyne receiver using dynamic holography in AlGaAs/GaAs photorefractive multiple quantum wells. The dynamic hologram acts as an adaptive beamsplitter that compensates wavefront distortions in the presence of speckle and requires no path-length stabilization. The photorefractive quantum wells have the unique ability to achieve maximum linear homodyne detection regardless of the value of the photorefractive phase shift by tuning the excitonic spectral phase. We achieve a root mean square noise-equivalent surface displacement of $6.7 \times 10^{-7} \text{ \AA}(\text{W/Hz})^{1/2}$. © 1998 American Institute of Physics.

[S0003-6951(98)02434-6]

Laser-based ultrasound^{1,2} is a promising nondestructive evaluation technique for remote sensing, manufacturing diagnostics, and in-service inspection for many industrial applications. It may also offer the potential for detecting ultrasonic signals from human tissue without the need for mechanical contact with the skin in conjunction with photoacoustic ultrasonography.³ Nonadaptive homodyne and heterodyne reference-beam interferometers have been used for ultrasound detection, but they often do not operate effectively with the speckle that results from interrogating rough surfaces. The development of time-delay interferometers (such as the confocal Fabry–Perot)⁴ allows the processing of light scattered from a rough surface with a large field of view, but requires path length stabilization of the interferometer length to a fraction of an optical wavelength. More recently, a number of laser ultrasonic receivers based on coherent detection using compensated reference-beam interferometers have been developed.^{5–10}

In this work we use photorefractive quantum well thin films^{11–13} as high-sensitivity¹⁴ holographic devices that operate at the extremely low light intensities compatible with the low light levels returned from typical surfaces under inspection. These devices act as adaptive beamsplitters to compensate wavefront distortions and do not require path length stabilization. Most importantly, the photorefractive quantum wells have a unique ability to achieve linear homodyne detection regardless of the value of the photorefractive phase shift. In this letter we show that this feature of the photorefractive quantum wells is a consequence of excitonic spectral phase.

The devices used in our experiments were grown by molecular beam epitaxy on semi-insulating GaAs substrates at

600 °C. The active electro-optic layers consisted of a multiple quantum well layer composed of a 100 period superlattice of 70 Å GaAs wells and 60 Å Al_{0.30}Ga_{0.70}As barriers with a total thickness of 1.3 μm. The superlattice was proton implanted after growth with two doses of $1 \times 10^{12} \text{ cm}^{-2}$ at energies of 80 and 160 keV to make them semi-insulating. The quantum wells were grown on a stop-etch layer of 5000 Å Al_{0.50}Ga_{0.50}As, which allowed the samples to be epoxied to glass and the substrate removed to perform optical transmission experiments. Titanium–gold coplanar contacts 4 mm long with a gap of 0.8 mm were evaporated to apply transverse electric fields to operate the quantum wells in the transverse Franz–Keldysh geometry.^{13–15}

The electro-optic spectra of the samples were characterized by measuring differential transmission $\Delta T/T$ as a function of the electric field and is shown in Fig. 1(a). The differential transmission approaches 120% at electric fields of 25 kV/cm. The change in absorption $\Delta\alpha$ due to the applied electric fields is shown in Fig. 1(b). We observed a large electroabsorption approaching 6000 cm^{-1} compared with a maximum absorption of the heavy-hole exciton of approximately $15\,000 \text{ cm}^{-1}$. The changes in the absorption spectrum are accompanied by changes in the refractive index in the material through the Kramers–Kronig transformations.¹⁶ The calculated change in the refractive index Δn is shown in Fig. 1(c). The fractional change in index $\Delta n/n$ approaches 1%. These large changes in the absorption and index are critical ingredients for good signal-to-noise detection in a homodyne interferometer during two-wave mixing.

A key figure of merit in evaluating the performance of an ultrasonic receiver is the noise equivalent surface displacement (NESD), which is the minimum surface displacement detectable for a signal-to-noise ratio equal to unity for a detection bandwidth (BW) and a power level P_h on the

^{a)}Electronic mail: nolte@physics.purdue.edu

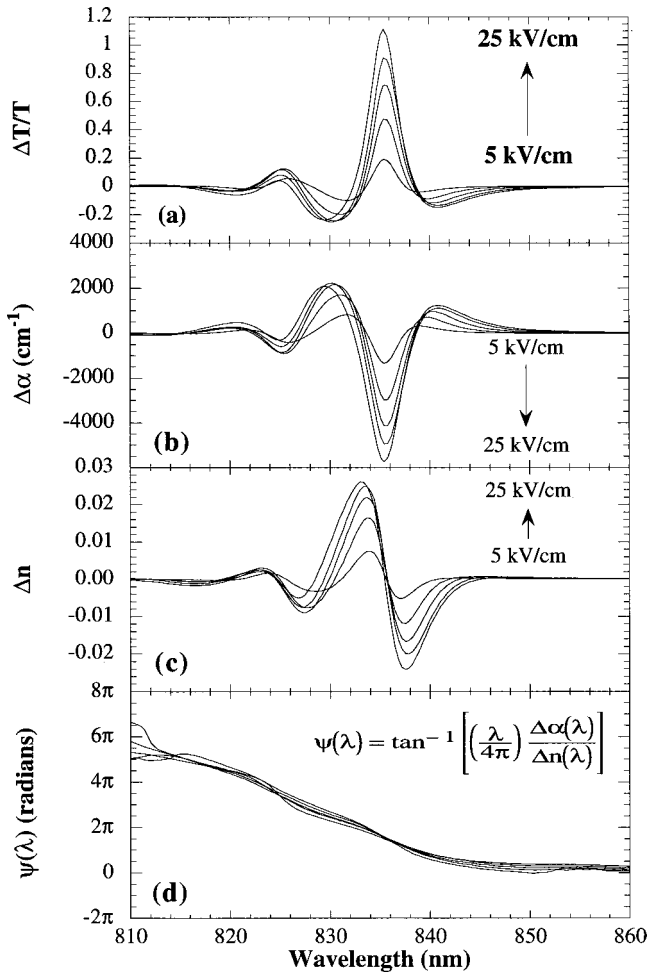


FIG. 1. The electro-optic response of the photorefractive quantum well for different transverse electric fields on device No. 101196D. Large changes in absorption $\Delta\alpha$ (b) and index Δn (c) guarantee efficient two-wave mixing. The changing spectral phase, $\psi(\lambda)$ shown in (d), allows tuning to quadrature to achieve linear detection.

detector. For a classical homodyne interferometer in the shot noise limit, the signal-to-noise is given by

$$\frac{S}{N} = \sqrt{\frac{2\eta P_h}{h\nu(BW)}} \frac{4\pi\delta}{\lambda}, \quad (1)$$

where η is the detector quantum efficiency, ν is the optical frequency, and δ is the root mean square (rms) surface displacement. The NESD for a classical homodyne interferometer for a bandwidth of 1 Hz and a power at the detector of 1 W is given as

$$\delta_{\text{lim}}^{\text{classic}} = \left(\frac{\lambda}{4\pi}\right) \sqrt{\frac{h\nu}{2\eta}}. \quad (2)$$

At a wavelength of 850 nm with $\eta=0.75$ the NESD is $\delta_{\text{lim}}^{\text{classic}} = 2.7 \times 10^{-7} \text{ \AA}(\text{W/Hz})^{1/2}$. A detection limit of $6.2 \times 10^{-6} \text{ \AA}(\text{W/Hz})^{1/2}$ has been demonstrated in bulk photorefractive CdTe:V crystals⁶ and the detection limit for the commonly used confocal Fabry–Perot interferometer in transmission is $3 \times 10^{-6} \text{ \AA}(\text{W/Hz})^{1/2}$ at the peak of the frequency response.¹⁷

Homodyne detection in photorefractive quantum wells depends on the phase relationship between the diffracted reference beam and the transmitted signal beam. In the limit of

small diffraction efficiency, the electric field of the superposed beam impinging on the detector is given by

$$E_h = \exp(-\alpha_0 L) \left[E_s + \sqrt{\eta(\lambda)} E_r \right] \times \exp\left(i\left(\phi_0 + \psi(\lambda) + \left(\frac{4\pi}{\lambda}\right)d(t) + \frac{\pi}{2}\right)\right), \quad (3)$$

where E_h , E_s , and E_r are the combined beam at the exit, the signal beam at the entrance, and the reference beam at the entrance of the photorefractive quantum well device, respectively, $d(t)$ is the time-dependent surface displacement, and $\eta(\lambda)$ is the quantum-well diffraction efficiency which is a function of wavelength and beam ratio. The photorefractive phase shift between the interference pattern and the recorded hologram is given by ϕ_0 . The excitonic spectral phase associated with the relative contributions of the index and absorption gratings to the combined beam is given by $\psi(\lambda)$

$$\psi(\lambda) = \tan^{-1}\left[\left(\frac{\lambda}{4\pi}\right) \frac{\Delta\alpha(\lambda)}{\Delta n(\lambda)}\right]. \quad (4)$$

The spectral phase $\psi(\lambda)$ is an approximately linear function in wavelength through the excitonic transitions,¹⁸ and is insensitive to the applied electric field as shown in Fig. 1(d). Optimal linear homodyne detection occurs at quadrature when the phase of the transmitted signal relative to the diffracted signal is equal to $\pi/2$ during two-wave mixing. The unique feature of the photorefractive quantum wells is that this condition can always be satisfied for any photorefractive phase shift by tuning the wavelength of the probe laser. Quadrature is satisfied when $\phi_0 = -\psi(\lambda)$, for which the signal-to-noise ratio in the signal-arm beam is

$$\frac{S}{N} = \frac{\eta\delta P_h/h\nu}{\sqrt{\eta P_h/h\nu} BW} \approx 2 \sqrt{\frac{\eta P_r}{h\nu BW}} \exp\left(-\frac{\alpha_0 L}{2}\right) \sqrt{\eta(\lambda)} \left(\frac{4\pi}{\lambda}\right) d(t), \quad (5)$$

where δP_h is the time-varying component of the total power. The noise-equivalent surface displacement (NESD) for the photorefractive multiple quantum well thin film is thus given by

$$\delta_{\text{min}}(\lambda) = \left(\frac{\lambda}{4\pi}\right) \frac{1}{2\sqrt{\eta(\lambda)}} \exp\left(\frac{\alpha_0 L}{2}\right) \sqrt{\frac{h\nu BW}{2\eta P_r}}. \quad (6)$$

The value of δ_{min} given by Eq. (6) is larger than the ideal value of Eq. (2) by

$$\frac{\exp[(\alpha_0 L/2)]}{2\sqrt{\eta(\lambda)}}.$$

We performed degenerate two-wave mixing on the devices to experimentally measure the NESD by writing a grating using a cw Ti sapphire laser with a fringe/grating spacing of $\Lambda = 300 \mu\text{m}$. The long fringe spacing was used as a convenience to study the physical behavior of mixing in the quantum wells, although more realistic fringe spacings of $20 \mu\text{m}$ or less could be used in practical systems. Homodyne measurements were performed using a piezoelectric trans-

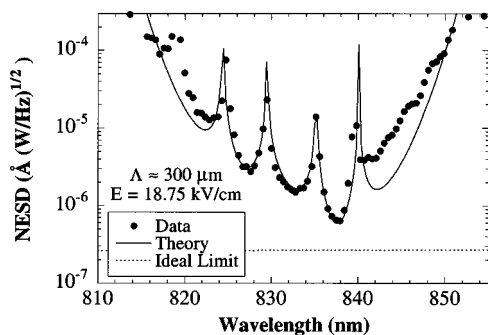


FIG. 2. The spectral dependence of the noise-equivalent-surface displacement, NESD, showing good agreement between theoretical prediction and experimentally measured values during two-wave mixing for an incident laser power of $20 \mu\text{W}$ on device No. 101196D.

ducer or an electro-optic phase modulator to simulate surface displacement, and a dc electric field was applied across the contacts. The transmitted signal was measured using a shot-noise-limited silicon photodetector with a 125 MHz bandwidth. The writing beams had nearly equal intensities in all mixing experiments.

The signal-to-noise ratio during homodyne mixing was measured using a spectrum analyzer with a 1 Hz bandwidth for an incident power of $20 \mu\text{W}$ on the device. The spectral dependence of the NESD of device No. 101196D is shown in Fig. 2 for an electric field of 18.75 kV/cm, compared with values of NESD that are predicted from Eq. (6) using the electroabsorption data of the same device from Fig. 1(b). Good agreement with the theoretical prediction is demonstrated, and a noise equivalent surface displacement of $6.7 \times 10^{-7} \text{ \AA}(\text{W/Hz})^{1/2}$ is measured, which is within a factor of 3 of ideal homodyne limit of Eq. (2). The NESD could be further improved by about a factor of two [see Eq. (5)] by increasing the power in the reference laser beam while keeping the power of the signal laser beam constant.

Figure 3 shows the temporal response of the homodyne signal for several different wavelengths demonstrating tuning through quadrature (required for linear detection) by tuning the wavelength of the probe laser. Homodyne detection

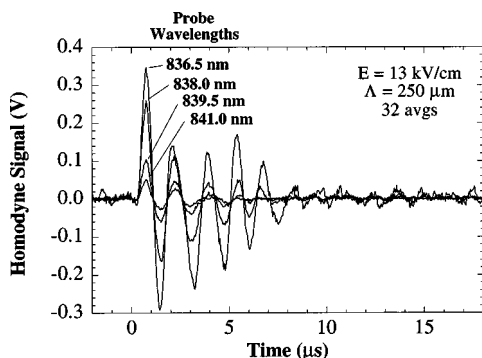


FIG. 3. The temporal response of the homodyne signal for different probe laser wavelengths on device No. 020197C. Tuning for optimal homodyne signal by adjusting the wavelength (to control the excitonic spectral phase) is demonstrated, which is unique to the photorefractive quantum wells.

was performed using an (EOSI) diode laser with a total incident power of $28 \mu\text{W}$. A 2 MHz underdamped piezoelectric transducer was used to vibrate the surface of a mirror which reflected the signal beam onto the photorefractive quantum well. The electric field applied to device No. 020197C was 16.8 kV/cm and the temporal signal was detected on a digital storage oscilloscope with 32 averages. The maximum homodyne signal was achieved at a wavelength of 836 nm, where the mixed waves achieve quadrature.

In conclusion we have demonstrated the operation of a novel laser-based ultrasound receiver based on two-wave mixing in photorefractive multiple quantum wells, operating close to the quantum noise limit. We have also demonstrated the ability to tune to quadrature by using the excitonic spectral phase. The tunability and sensitivity of these devices make them viable candidates for applications in industrial markets.

This research is supported in part by the Materials Research Science and Engineering Center program of the National Science Foundation (NSF) under award No. DMR-9400415. D. D. Nolte acknowledges support by NSF Grant No. ECS-9708230. L. J. Pyrak-Nolte acknowledges support from the NSF Young Investigator Award from Earth Sciences Division. M. R. Melloch acknowledges support from U. S. Air Force Office of Scientific Research F49620-96-1-0234A. Dr. Kruger's work is supported in part by NIH Grant No. CA65744. M. B. Klein acknowledges support from the NSF SBIR program under award No. 9660966.

- ¹C. B. Scruby and L. E. Drain, *Laser Ultrasonics: Techniques and Applications* (Adam Hilgar, Bristol, 1990).
- ²J.-P. Monchalain, *Review of Progress in Quantum Nondestructive Evaluation*, edited by D. O. Thompson and D. Chimenti (Plenum, New York, 1993), Vol. 12, pp. 495–506.
- ³R. A. Kruger, P. Y. Liu, Y. Fang, and C. R. Appledorn, *Med. Phys.* **22**, 1605 (1995).
- ⁴J.-P. Monchalain, R. Heon, P. Bouchard, and C. Padiou, *Appl. Phys. Lett.* **55**, 1612 (1989).
- ⁵A. Blouin and J.-P. Monchalain, *Appl. Phys. Lett.* **65**, 932 (1994).
- ⁶L.-A. de Montmorillon, I. Biaggio, P. Delaye, J.-C. Launay, and G. Roosen, *Opt. Commun.* **129**, 293 (1996).
- ⁷D. M. Pepper, G. J. Dunning, P. V. Mitchell, S. W. McCahon, M. B. Klein, and T. R. O'Meara, *Proc. SPIE* **2703**, 91 (1996).
- ⁸M. P. Petrov, S. I. Stepanov, and G. S. Trofimov, *Sov. Tech. Phys. Lett.* **12**, 379 (1986).
- ⁹I. A. Sokolov and S. I. Stepanov, *J. Opt. Soc. Am. B* **10**, 1483 (1993).
- ¹⁰S. I. Stepanov, *Appl. Opt.* **33**, 915 (1994).
- ¹¹D. D. Nolte, D. H. Olson, G. E. Doran, W. H. Knox, and A. M. Glass, *J. Opt. Soc. Am. B* **7**, 2217 (1990).
- ¹²D. D. Nolte, M. R. Melloch, J. M. Woodall, and S. E. Ralph, *Appl. Phys. Lett.* **61**, 3098 (1992).
- ¹³D. D. Nolte and M. R. Melloch, *Photorefractive Effects and Materials*, edited by D. D. Nolte (Kluwer, Dordrecht, 1995), pp. 373–451.
- ¹⁴Q. N. Wang, R. M. Brubaker, D. D. Nolte, and M. R. Melloch, *J. Opt. Soc. Am. B* **9**, 1626 (1992).
- ¹⁵Q. N. Wang, D. D. Nolte, and M. R. Melloch, *Appl. Phys. Lett.* **59**, 256 (1991).
- ¹⁶I. Pankove, *Optical Processes in Semiconductors* (Dover, New York, 1971).
- ¹⁷P. Delaye, A. Blouin, D. Drolet, L.-A. DeMontmorillon, G. Roosen, and J.-P. Monchalain, *J. Opt. Soc. Am. B* **14**, 1723 (1997).
- ¹⁸Y. Ding, D. D. Nolte, M. R. Melloch, and A. M. Weiner, *IEEE J. Sel. Top. Quantum Electron.* **4**, 332 (1998).